Scaling properties of phase change nanostructures and thin films

Simone Raoux[1]*, Charles T. Rettner[1], Jean L. Jordan-Sweet[2], Vaughn R. Deline[1], Jan Boris Philipp[3], and Hsiang-Lan Lung[4]
IBM Macronix Infineon PCRAM Joint Project

1. IBM Almaden Research Center, 650 Harry Road, San Jose, California 95120
   *e-mail: simone_raoux@almaden.ibm.com
2. IBM T. J. Watson Research Center, P. O. Box 218, Yorktown Heights, New York 10598
3. Infineon Technologies, IBM T. J. Watson Research Center, Yorktown Heights, New York 10598
4. Macronix International Co. Ltd., IBM T. J. Watson Research Center, Yorktown Heights, New York 10598

ABSTRACT

The scaling behavior of phase change materials is important for their application in solid state memory devices. We have studied the scaling behavior of ultra-thin films and nanostructures using time-resolved X-ray diffraction (XRD). Ultra-thin films of the phase change materials $Ge_2Sb_2Te_5$ (GST) and GeSb having thicknesses between 1 and 20 nm were deposited by magnetron sputtering and the crystallization behavior as a function of film thickness was investigated. We observed that the minimum thickness for the appearance of XRD peaks is a function of the phase change material. For GST the amorphous-fcc phase transition temperature increases with decreasing film thickness, and for 3.6nm and thinner films the fcc phase does not form anymore. The hcp phase is still observed for films as thin as 2 nm at about the same temperature as for hick films (about 370ºC), and it is not formed anymore for 1.5nm thick films. For GeSb XRD peaks (hcp phase) were observed for films as thin as 1.3 nm with an increased crystallization temperature T_x for the thinnest films.

Electron-beam lithography was used to fabricate nanostructures of amorphous GeSb having diameters between 20 and 55 nm with spacings between 80 and 100 nm over a 2mmx5mm field which was larger than the X-ray beam. Using time-resolved XRD we found that the amorphous to hexagonal phase transition occurs for all GeSb nanopatterns down to 20nm diameter. For the first time size effects are observed for T_x which decreased with particle size (by about 20 deg for the smallest particles compared to T_x for blanket films). The temperature range over which the transition occurs is also broadened compared to blanket film probably caused by the slight size variation from particle to particle and the size-dependent T_x. The XRD peaks of the nanopatterns are at the same angles as those for blanket films, but the XRD spectra show a difference in crystallographic texture.

Key words: scaling, phase change nanostructures, phase change thin films, XRD

1. INTRODUCTION

Solid state memory devices based on phase change materials (PCM) as the storage medium have been developed over the last years with ever shrinking dimensions. These devices exploit the large difference between the resistivity of the amorphous and crystalline phases of PCM to store information. The possibility to change the phase of the PCM repeatedly between the two phases has been demonstrated in devices with an endurance of up to 10^{12} times[1]. To switch from the amorphous to the crystalline phase (SET), the PCM in the device is heated by an electrical current for a long enough time above the crystallization temperature, and to switch from the crystalline to the amorphous phase (RESET) the material is melt-quenched by a larger current with a very short trailing edge that leads to melting and subsequent quenching of the PCM in the amorphous phase. Phase change solid state memory shows favorable properties with respect to scaling because smaller devices require a smaller current to RESET the devices, which is one of the limiting factors for the size of the transistor that is required to switch the cells. Various materials have been described to perform well in solid state memory devices such as $Ge_2Sb_2Te_5$ (GST)[1,2], nitrogen[3], oxygen[4], tin[5], or silicon[6] doped GST, and doped Sb_2Te[7]. Little is known how scaling in either 2D (just film thickness) or 3D (phase change nanoparticles) influences the crystallization behavior, even though this information is of crucial importance to estimate the scalability of this technology. In this paper we investigate the crystallization behavior of ultra-thin PCM

films and large arrays of PCM nanoparticles fabricated by electron beam lithography, and compare their crystallization behavior to thick PCM films.

2. EXPERIMENTS

PCM thin films were deposited by magnetron sputtering using stoichiometric $Ge_2Sb_2Te_5$ and Ge(15%)Sb(85%) sputter targets. The substrates were Si wafers (for Secondary Ion Mass Spectrometry (SIMS) measurements) or Si wafers coated with a 1 μm thick thermal oxide. A major concern for the studies of very thin films is oxidation. Figure 1 shows the SIMS data on uncapped GeSb and GST films exposed to air for several days between the deposition and the SIMS measurement.

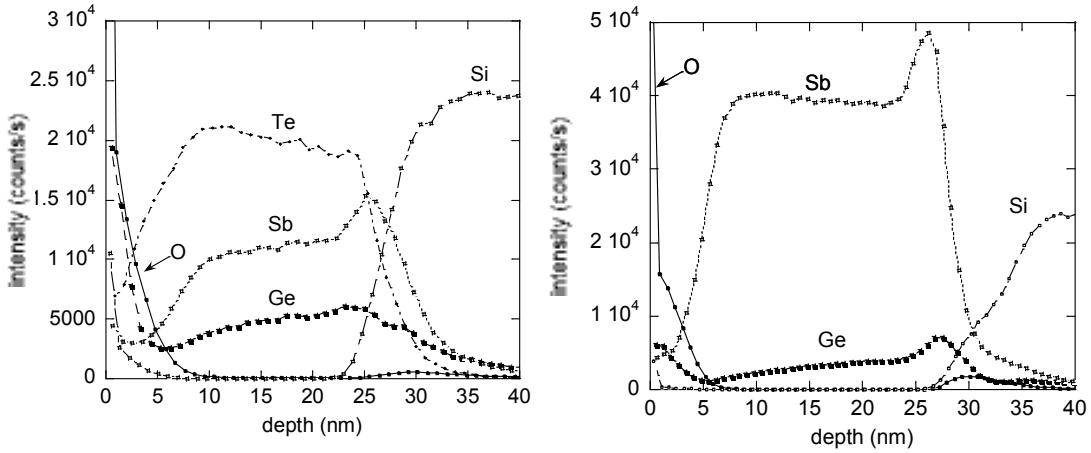

Fig. 1: SIMS depth profiles on uncapped GST (left) and GeSb (right) films exposed to air for several days between the deposition and the SIMS measurement.

It is clear that the top about 5nm of the films contain a large amount of oxygen. In addition we observe that the film composition is markedly different at the interface with peaks in the Ge and Sb concentration and a depletion of the Te concentration (for GST). We have found previously that very thin films basically do not show any bulk-like concentration behavior with a fixed composition over some depth range but vary their composition continuously throughout the film[8]. In order to study the properties of ultra-thin films of a few nm it is necessary to prevent oxidation. We applied a 10nm Al_2O_3 cap layer on top of a 30nm GeSb thin film *in situ* and exposed an uncapped and a capped sample to a 1h UV-ozone treatment. This treatment accelerates the film oxidation, SIMS depth profiling of the uncapped film showed that the top about 10nm of the film contained a large amount of oxygen. Figure 2 shows the ellipsometry raw data of the uncapped and capped GST film before and after UV-ozone treatment. The UV-ozone treatment has clearly modified the optical properties of the uncapped GST films, but the GST/ Al_2O_3 bilayer has nearly identical optical properties before and after UV-ozone treatment. We did not attempt to model these films since this requires a detailed knowledge about their respective thicknesses and the optical properties of all materials including the oxidized GST which also probably vary as a function of oxygen concentration. We just used ellipsometry to demonstrate that in the uncapped case the film changed dramatically under UV-ozone treatment while in the capped case the bilayer structure essentially did not change its optical properties. The results for capped and uncapped GeSb were very similar. We also did not attempt to sputter depth profile the Al_2O_3 capped PCM since we have experienced that sputter depth profiling of a bilayer that consists of a layer with a very low sputter rate (e.g. Ta or Al_2O_3) on top of a layer with a very high sputter rate (e.g. GST and GeSb) leads to the formation of very strong topographic features due to preferential sputtering. This strong topography leads to that fact that sputter time cannot be equaled to depth information anymore, and sputter depth profiling is not an adequate means to study these bilayers.

We deposited thin films of GST and GeSb with thicknesses between 1 and 20nm sandwiched between two 10nm thick Al_2O_3 layers for all the subsequent experiments.

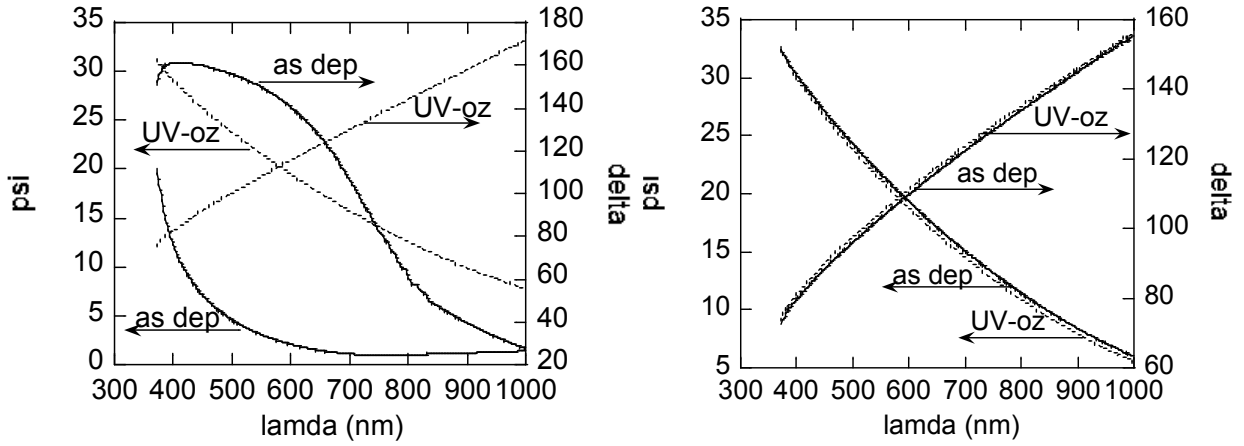

Fig. 2: Ellipsometry raw data (psi and delta) of the uncapped (left) and 10nm Al_2O_3 capped (right) GST film before and after UV-ozone treatment.

The film thickness of the ultra-thin films was determined by ellipsometry after fitting the optical constants for each material using a thick film for which the film thickness was determined by profilometry.

GeSb nanostructures were fabricated using electron beam lithography from a 50nm thick film deposited on 1 μm-thick SiO_2 on Si substrates. The patterns were made using 950k PMMA resist. In order to minimize any annealing of the samples, the resist was only baked to 105^{o}C, which is just above the glass transition temperature of the PMMA. The nanostructures extended over an area of 2mmx5mm that was larger than the x-ray probe beam of the time-resolved X-ray diffraction (XRD) set-up. Fig. 3 shows SEM images of the nanostructures.

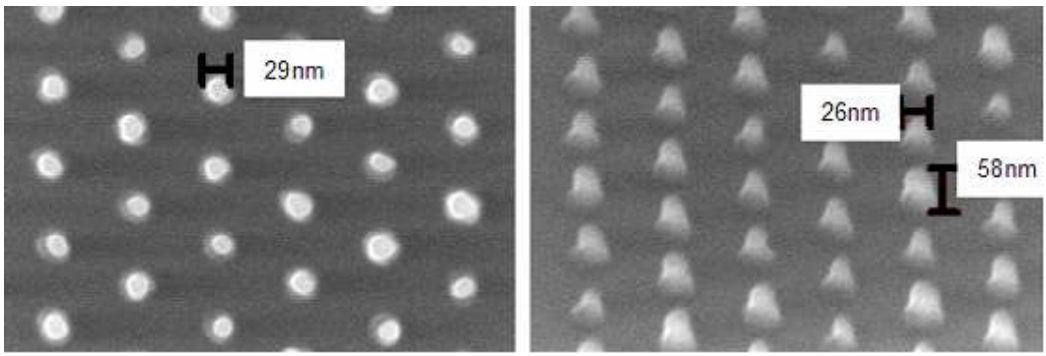

Fig. 3: Secondary Electron Microscopy (SEM) images of GeSb nanostructures. Top view (left) and view at 45 deg (right).

The nanostructures were also encapsulated *in situ* using 10nm Al_2O_3 deposited at an angle of 45 deg, thus the actual size of the PCM inside the patterns is about 10nm smaller than the total size as measured by SEM.

Time-resolved *in-situ* x-ray diffraction (XRD) was employed to study the structural properties of capped ultra-thin films and nanostructures. These experiments were performed at beamline X-20C of the National Synchrotron Light Source using a photon energy of 6.9 keV. The set-up consisted of a high-throughput synthetic multilayer monochromator and fast linear-diode-array detector[9,10]. A special chamber for controlling the sample ambient (purified He gas) was outfitted with a BN heater for rapid annealing up to 1200ºC at a rate of ≤ 35ºC/sec.[11,12]

3. RESULTS & DISCUSSION

Thin GST films were heated in a helium atmosphere and the intensity of the XRD peaks was recorded over a 2 theta range of 15 degrees. The range was selected to cover strong XRD peaks of this material. Bulk GST and relatively thick films are known to show an amorphous-fcc phase transition at around 140ºC and an fcc-hcp phase transition at around 360ºC[13]. Fig. 4 shows how the first, amorphous-fcc phase transition develops as a function of film thickness.

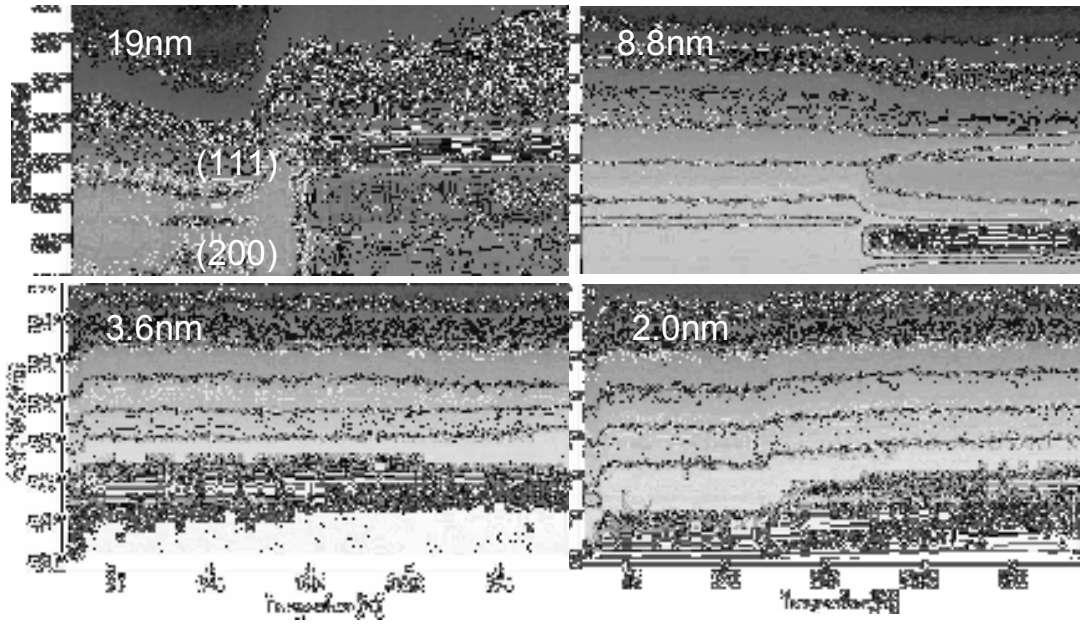

Fig. 4: XRD peak intensity as a function of temperature for thin GST films. Films heated to 280ºC at 1ºC/s.

The films were heated at a rate of 1ºC /s up to 280ºC. The 19nm thick film shows the amorphous-fcc phase transition at around 140ºC comparable to literature values[13]. For thinner films (8.8nm) the transition occurs at a higher temperature around 170ºC and the film texture changes. For thinner films we only observe very weak crystallization peaks.

The effect is different for the fcc-hcp phase transition as shown in Fig. 5. The hcp phase forms for all films including films as thin as 2 nm at a temperature of around 370ºC similar to literature values[13]. We observe again, for the samples heated to higher temperatures, what we found for samples heated up to 280ºC. The amorphous-fcc phase transition is shifted to higher temperatures as films become thinner, and it does not form anymore for 3.6nm and thinner films. We observe a direct transition from the amorphous to the hcp phase. This is quite surprising since the amorphous and fcc phases are so similar while the hcp phase is very complicated and requires 9 layers of atoms to arrange in the correct sequence. The c-axis of the hcp unit cell (c=1.7nm)[13] almost becomes comparable to the film thickness. For GST nanostructures we observed the opposite effect in an earlier experiment[14]: the amorphous-fcc phase transition occurred at the same temperature for nanostructures and blanket films around 140ºC , but the fcc-hcp transition was moved to higher temperatures for nanostructures compared to blanket (relatively thick, 50nm) films. The thinnest GST films (1.5nm) investigated in the present study did not show any XRD peaks when heated up to 430ºC.

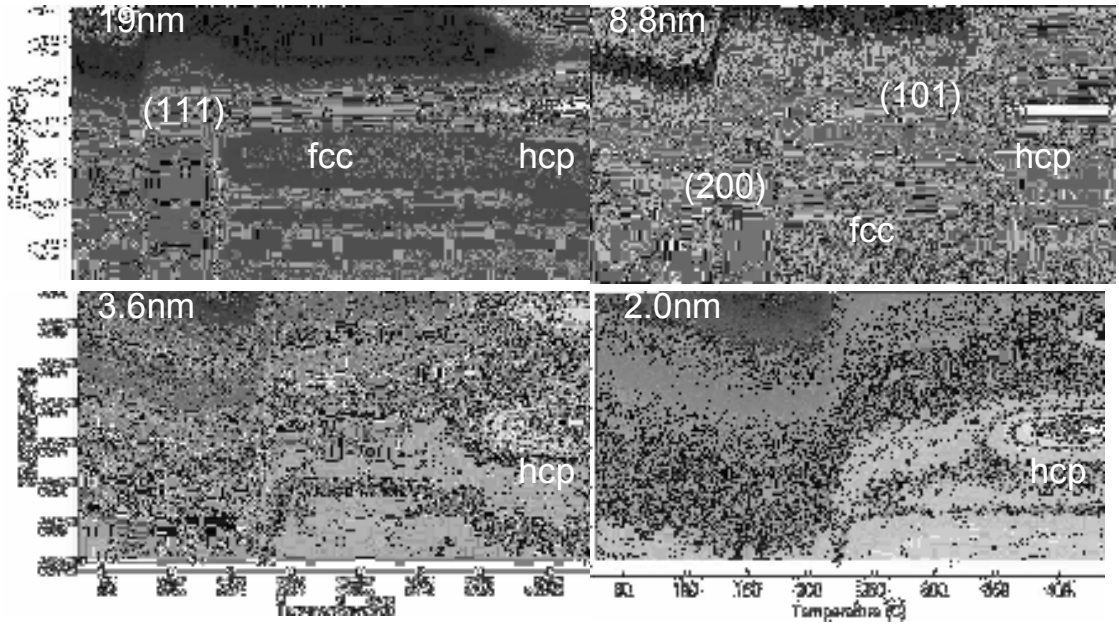

Fig. 5: XRD peak intensity as a function of temperature for thin GST films. Films heated to 430ºC at 1ºC/s.

Figure 6 shows the theta-2theta scans of GST films after annealing to 280ºC and to 430ºC. The resolution of these scans is relatively low and the line width is determined by the experimental set-up.

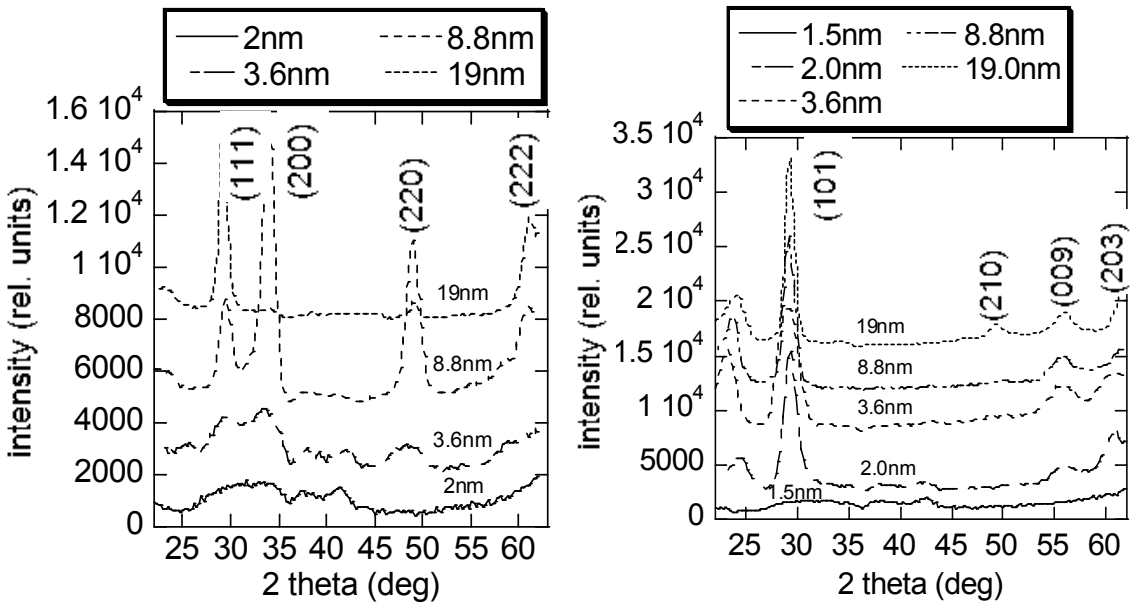

Fig. 6: Theta-2theta scans of GST films after annealing to 280ºC (left) and to 430ºC (right).

We can observe again as in the time-resolved studies that the fcc peaks become very weak when the film thickness is reduced, and that films of 2nm practically do not show any fcc peaks anymore, while they still show strong hcp peaks.

We investigated also a series of thin GeSb films. Figures 7 and 8 show the results.

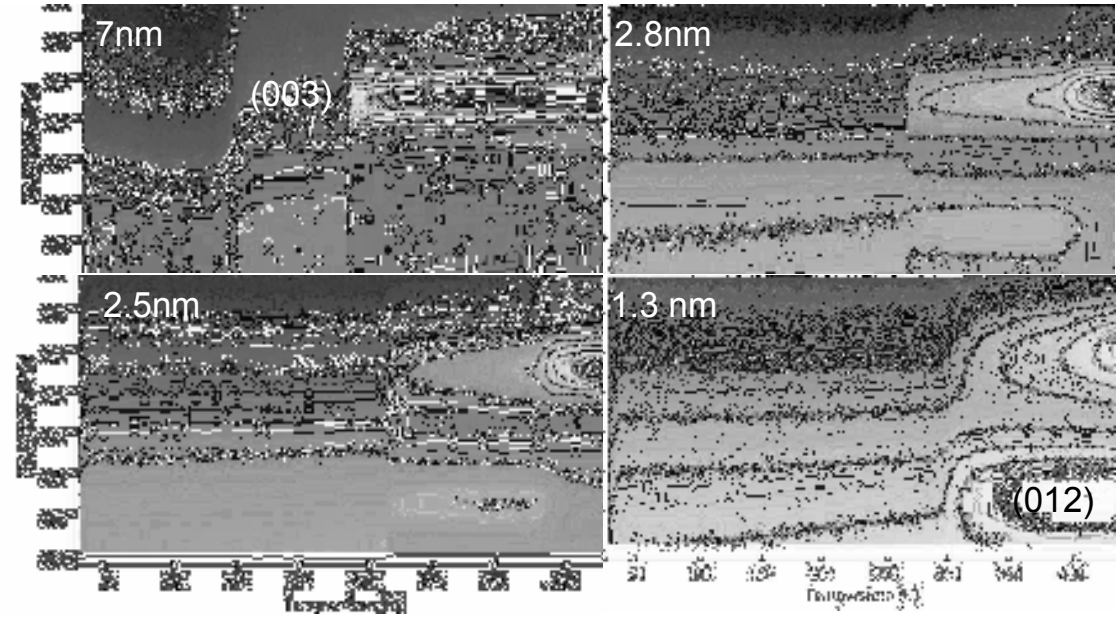

Fig. 7: XRD peak intensity as a function of temperature for thin GeSb films. Films heated to 430ºC at 1ºC/s.

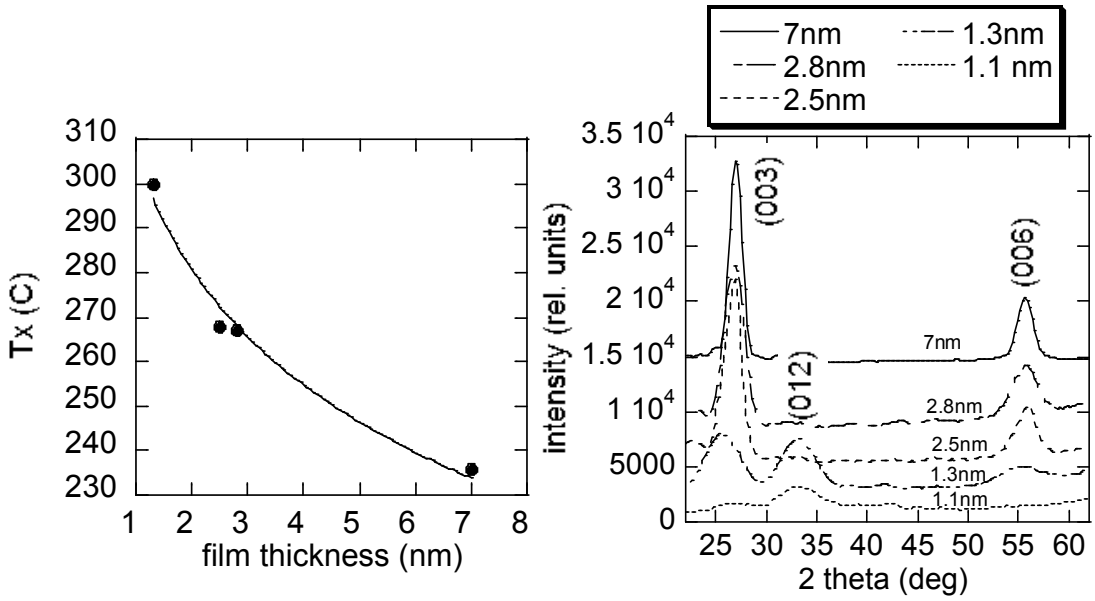

Fig. 8: Transition temperature as a function of films thickness (left) and the theta-2theta scans for thin GeSb films after being heated to 430ºC (right).

GeSb crystallizes similarly to pure Sb in the hcp phase with slightly different lattice parameters. The transition for the 7nm thick film is very sharp and occurs at about 240ºC, slightly lower than we have reported for thicker films of 50 nm (255ºC)[14]. This might be due to that fact that the thicker film was not capped. It is known from the literature that capping layers can influence the crystallization temperature T_x, and both, increased and decreased T_x have been observed depending on the PCM and the cap layer material. We need to further investigate what effect an Al_2O_3 cap layer has on T_x of GeSb. We find that with decreasing film thickness T_x is increased and the transition become broader and extent over a larger temperature range. The theta-2theta scans indicate that even the thinnest film (1.1nm) shows very weak diffraction peaks.

GeSb nanostructures were also studied. Results are shown in Figs. 9 and 10.

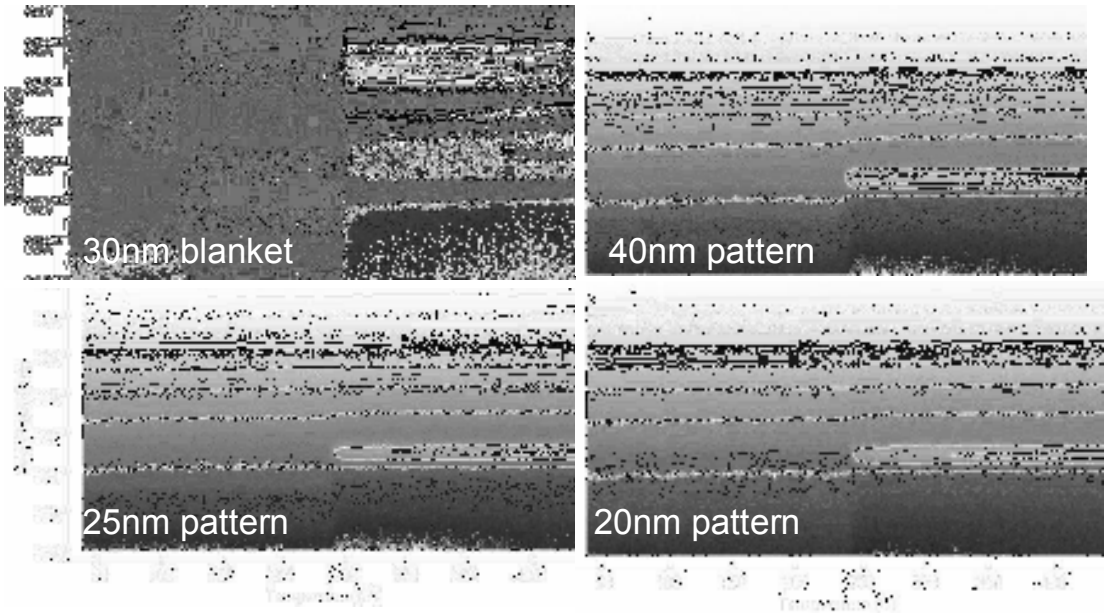

Fig. 9: XRD peak intensity as a function of temperature for GeSb blanket film (uncapped) compared to nanostructures. Films and nanostructures heated to 430ºC at 1ºC/s.

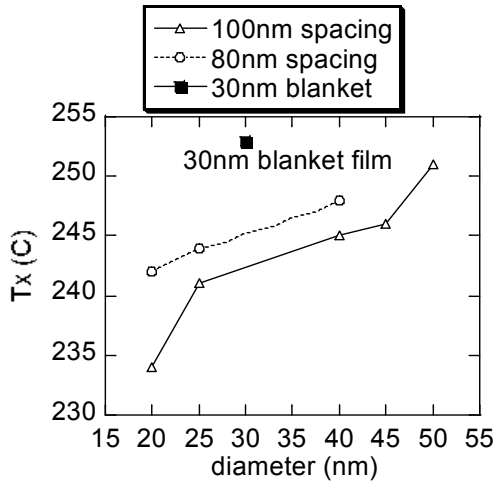

Fig. 10: Crystallization temperature as a function of pattern size for GeSb nanostructures.

We observed that all nanopatterns showed a clear sign of crystallization. The size of the nanopatterns ranged from 20-55 nm and the spacing was either 80 or 100nm. Here we found a small decrease of crystallization temperature with decreased nanoparticles size. This is the first time that we observe size effects caused by the nanopatterning. In previous experiments with nanopatterns of 60nm or larger the crystallization temperature of the nanopatterns agreed with that of blanket films[14]. For the (uncapped) 30nm thick reference film we find a transition temperature of about 253ºC, similar to the previously reported 50nm thick films. The theta-2theta scans after annealing of the nanostructures show no size-dependent change in peak position of the nanostructures compared to blanket films, but a difference in texture, as it is evident also from Fig. 9.

The transition also becomes broader for smaller nanostructures, while it occurs over about 5deg for blanket film it occurs over a temperature range of 10-20 deg for the nanostructures.

We investigated the ultra-thin films and nanostructures after heating using SEM and did not find any signs of agglomeration in the films or deterioration of the nanostructures.

4. CONCLUSION

The scaling behavior of phase change thin films and nanostructures has been studied using time-resolved XRD. Thin films of GST and GeSb as well as GeSb nanostructures were investigated. Thin films of GST (19nm) show the amorphous-fcc phase transition at around 140ºC comparable to bulk GST. For thinner films (8.8nm) the transition occurs at a higher temperature around 170ºC and for films of 3.6nm or thinner the fcc phase practically does not form. The hcp phase however forms for all films including films as thin as 2nm at a temperature of around 370ºC similar to bulk GST. The thinnest GST films (1.5nm) investigated in the present study did not show any XRD peaks when heated up to 430ºC. For GeSb thin films we observe an increase in T_x with decreasing films thickness, while on the other hand GeSb nanostructures showed a small decrease in T_x as the nanostructure size decreases. Films thicker than 1.1nm show the crystalline hcp phase, and all nanostructures we investigated with sizes between 20 and 55nm also showed clearly the crystalline phase. All these experiments indicate that scaling properties need to be measured really as a function of PCM and also its environment (e.g., encapsulation or capping material). Both thin films and nanostructures show a size dependent change in T_x, but none of the materials investigated here had a strong reduction in T_x that would have implications on data retention in devices. Very thin films and small nanostructures showed still clear crystallization which is an encouraging result regarding the scaling of phase change memory technology.

ACKNOWLEDGEMENTS

This research was carried out in part at The National Synchrotron Light Source, Brookhaven National Laboratory, which is supported by the U.S. Department of Energy, under Contract No. DE-AC02-98CH10886.

REFERENCES

1. S. Lai, IEDM Tech. Dig., 2003.
2. A. Pirovano, A. L. Lacaita, A. Benvenuti, F. Pellizzer, S. Hudgens, and R. Bez, IEDM Tech. Dig., 2003.
3. S. J. Ahn, Y. N. Hwang, Y. J. Song, S. H. Lee, S. Y. Lee, J. H. Park, C. W. Jeong, K. C. Ryoo, J. M. Shin, J. H. Park, Y. Fai, J. H. Oh, G. D. Koh, G. T. Jeong, S. H. Joo, S. H. Choi, Y. H. Son, J. C. Shin, Y. T. Kim, H. S. Jeong, and Kinam Kim, 2005 Symp. VLSI Technology Dig. Techn. Papers, p. 98
4. M. Matsuzaki, K. Kurotsuchi, Y. Matsui, O. Tonomura, N. Yamamoto, Y. Fujisaki, N. Kitai, R. Takemura, K. Osada, S. Hanzawa, H. Moriya, T. Iwasaki, T. Kawahara, N. Takaura, M. Terao, M. Matsuoka, and M. Moniwa, IEDM Tech.Dig., 2005.
5. S. L. Cho, H. Hoorii, J. H. Park, J. H. Yi, B. J. Kuh, Y.H.Ha, S. O. Park, H. S. Kim, U. I. Chung, and J. T. Moon, *European Symp. Phase Change and Ovonic Sci.,* Balzers, Lichtenstein, 2004
6. Y. C. Chen, H. P. Chen, Y. Y. Liao, H. T. Lin, L. H. Chou, J. S . Kuo, P. H. Chen, S. L. Lung, and R. Liu, *2003 Int. Symp. VLSI Technology, Systems and Applications,* Proc. Techn. Papers, Hsinchu, Taiwan, p. 32
7. M. Lankhorts, B. S. M. M. Ketelaars, and R. A. M. Wolters, Nature Mat. **4**, 347 (2005)
8. F. Houle, , S. Raoux, R. Shelby, A. Kellock, V. Deline and C. T. Rettner, MRS Spring Meeting, San Francisco, April 2006
9. G. B. Stephenson, Nucl. Instrum. Meth. Phys. Res. A **266**, 447 (1988)
10. G. B. Stephenson, K. F. Ludwig, Jr., J. L. Jordan-Sweet, S. Brauer, J. Mainville, Y. S. Yang, and M. Sutton, Rev. Sci. Instrum. **60**, 1537 (1989)
11. L.A. Clevenger, R.A. Roy, C. Cabral, Jr., K.L. Saenger, S. Brauer, G. Morales, K.F. Ludwig, Jr., G. Gifford, J. Bucchignano, J. Jordan-Sweet, P. DeHaven, and G.B. Stephenson, J. Mater. Res. **10**, 2355 (1995)
12. C. Lavoie, C. Cabral, Jr., L.A. Clevenger, J.M.E. Harper, J. Jordan-Sweet, K.L. Saenger, and F. Doany, Mater. Res. Soc. Symp. Proc. **406**, 163 (1996).
13. I. Friedrich, V. Weidenhof, W. Njoroge, P. Franz, and M Wuttig, J. Appl. Phys. **87**, 4130 (2000)
14. S. Raoux, C. T. Rettner, J. L. Jordan-Sweet, M. Salinga, and M. F. Toney, EPCOS 05, paper 14, Cambridge, September 2005.